New Degrees of Freedom using N_{eff} (Effective Neutrino Species) measurements of CMB

Prakhar Bansal

Advisor: **Adam Ritz**
University of Victoria, Canada

Contents

1. N_{eff} in Standard Model

1.1 Thermal History of the Neutrinos

The primordial universe was a hot, dense soup of particles smashing into each other, forming new particles. As the universe expanded and temperatures dropped down, the interaction rates of many of these particles couldn't keep up with the expansion rate (Hubble's rate), and they dropped out of equilibrium from the Standard Model (SM) plasma consisting of electrons, protons, positrons and photons. Owing to the weak nature of neutrino interactions with the electrons, neutrinos dropped out way early (T $\sim$ 1 MeV; t $\sim$ 1s) as compared to the photons (T $\sim 10^{-7}$ MeV; t $\sim$ 380,000 years), which are coupled tightly by Electromagnetic Thomson Scatterings.

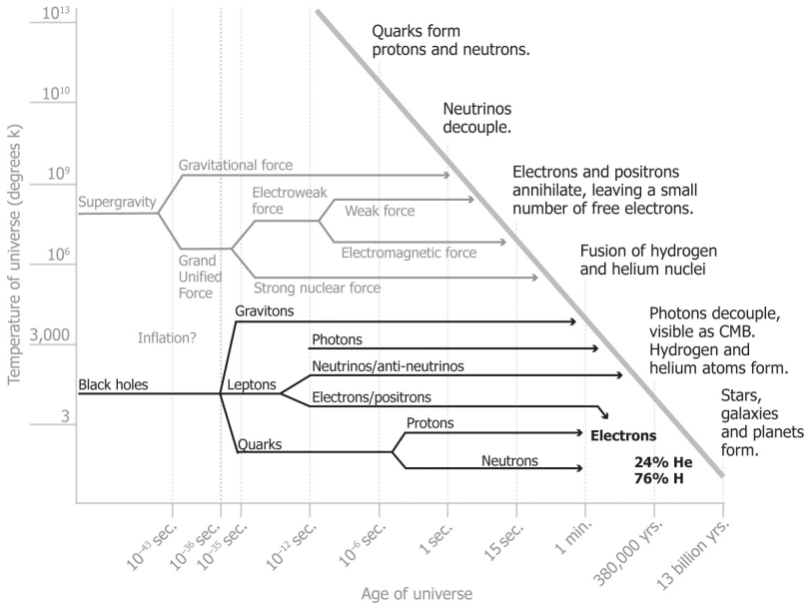

Figure 1.1: Credits: Loosing the Nobel Prize, Brian Keating

At early times, particle interactions were efficient enough to keep the different species in local equilibrium. They then shared a common temperature T, and the distribution functions take their maximum entropy Bose-Einstein (bosons) and Fermi-Dirac (fermions) forms. The energy density

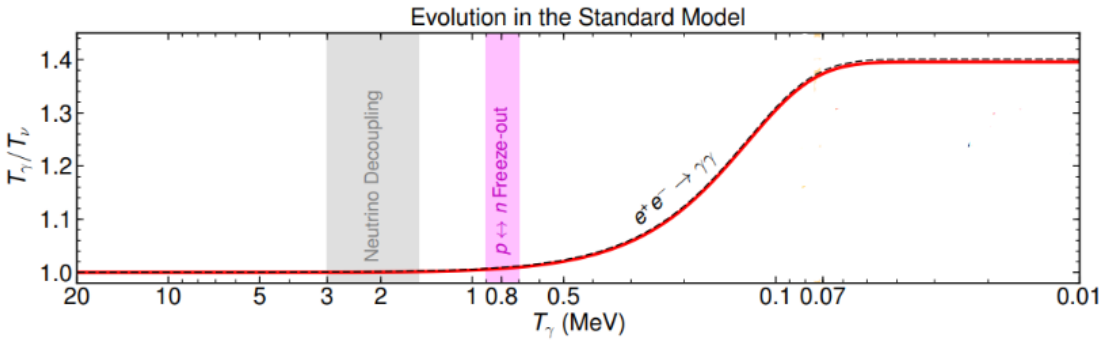

Figure 1.2: T_γ vs T_ν in SM

of a species in such scenario is given by [1]

$$\rho_a = g_a \int \frac{d^3p}{2\pi^3} \frac{E(p)}{e^{(E_a-\mu_a)/T} - 1} \tag{1.1}$$

where g_a are the internal degrees of freedom of a species and μ_a is the chemical potential, which is usually small for photons and other species. So, we'll neglect it for now in our calculations but will revisit the significance of chemical potential in later chapters.

For a massless species E(p) = p, thus we obtain

$$\rho_a = \begin{cases} \frac{\pi^2}{15} T_a^4 & \text{(boson)} \\ \frac{7}{8}\frac{\pi^2}{15} T_a^4 & \text{(fermion)} \end{cases} \tag{1.2}$$

We want to track the neutrino energy density, which can be expressed as

$$\rho_\nu = 3 \times \frac{7}{8} \frac{T_\nu^4}{T_\gamma^4} \rho_\gamma \tag{1.3}$$

where the factor of 3 is because of three neutrino flavours

The above equation tells us that the neutrino energy density can be tracked effectively if we know how the Temperature of neutrinos vary as compared to the photons. From the time of Big Bang till neutrinos decoupled, neutrinos and photons shared a common temperature as neutrinos were coupled to the SM plasma. Shortly after neutrinos decoupled, electron-positron annihilations pumped energy into the photons but neutrinos, being decoupled, already received almost none of this energy.

A naive calculation of the photon temperature following the electron-positron annhiliations can be done using the entropy conservation arguments which is true under the adiabatic evolution of universe.

The entropy density of any species is defined as

$$s = \frac{\rho + P}{T} \tag{1.4}$$

where P is the pressure of the species

For a relativistic species P = $\rho/3$

The entropy density of a massive particle (m » T) is negligible as bth ρ and P are exponentially suppressed. At the temperatures around neutrino decoupling massive species like electrons and positrons are also relativistic (T » m). Thus the total entropy density before the annhiliations is

$$s_i = 3s_\nu + s_\gamma + s_{e^-} + s_{e^+} \tag{1.5}$$

$$s_i = \frac{4}{3}\left(3 \times 2 \times \frac{7}{8}\frac{\pi^2}{15}T_\nu^3 + 2 \times \frac{\pi^2}{15}T_\gamma^3 + 4 \times \frac{7}{8}\frac{\pi^2}{15}T_\gamma^3\right)(T_{e^-} = T_{e^+} = T_\gamma) \tag{1.6}$$

Before annihilation, at a scale factor a_i, the neutrinos are coupled with SM tightly and thus $T_\nu = T_\gamma = T_i$

$$\implies s_i = \frac{4\pi^2}{45} \times \frac{43}{4}T_i^3 \tag{1.7}$$

After the annihilation, we are left with only photons and neutrinos at different temperatures

$$\implies s_f = \frac{4\pi^2}{45}\left(6 \times \frac{7}{8}T_\nu^3 + 2T_\gamma^3\right) \tag{1.8}$$

Conserving the total entropy $s(a)a^3$ before and after annhiliations we get

$$s_i a_i^3 = s_f a_f^3 \tag{1.9}$$

Once neutrinos are decoupled, their temperature simply scales as $T \propto a^{-1}$, as they are relativstic particles

$$\implies T_i a_i = T_\nu a_f \tag{1.10}$$

$$\implies T_\gamma^3 = \frac{11}{4}T_\nu^3 \tag{1.11}$$

Substituting this back into 1.3, we get

$$\rho_\nu = 3 \times \frac{7}{8}\left(\frac{4}{11}\right)^{4/3}\rho_\gamma \tag{1.12}$$

Assumption: The above analytic calculation assumes the neutrinos **instantaneously decouple** from the SM plasma at $T = T_i$ ($\implies T_i a_i = T_\nu a_f$). However the process of neutrino decoupling is gradual process. Hence the above equation needs to be corrected by letting go of the **instantaneous decoupling** assumption.

1.2 N_{eff} definition in Standard Model

The above problem can be reformulated by defining a quantity

$$N_{\text{eff}} = \frac{8}{7}\left(\frac{11}{4}\right)^{4/3}\frac{\rho_\nu}{\rho_\gamma} \tag{1.13}$$

As we can see in the case of instantaneous decoupling, the above equation yields $N_{\text{eff}} = 3$. N_{eff} is a measure of extra relativistic species in the Early Universe. In the next section, we'll see how we can numerically track the energy densities of neutrinos and photons to work out N_{eff}

1.3 Numerical Calculation: Escuedero's Code

1.3.1 The Liouville Equation

The distribution function f determines the thermodynamics of any given species in the early Universe. In a fully homogeneous and isotropic Universe, the time evolution of the distribution function f is governed by the Liouville equation

$$\frac{\partial f}{\partial t} - Hp\frac{\partial f}{\partial p} = \mathscr{C}[f] \tag{1.14}$$

where p is the momentum, H is the Hubble rate, and $\mathscr{C}[f]$ is the collision term which depends on the interactions of the given species.

Once the distribution function is determind the number density, energy and pressure density of a species are given by

$$n_a = g_a \int \frac{d^3p}{2\pi^3} f_a \tag{1.15}$$

$$\rho_a = g_a \int \frac{d^3p}{2\pi^3} E(p) f_a \tag{1.16}$$

$$\mathscr{P}_a = g_a \int \frac{d^3p}{2\pi^3} \frac{p^2}{3E(p)} f_a \tag{1.17}$$

1.3.2 Approximations

The actual solution to the Liouville equation 1.14 strongly depends upon the processes that the given species is undergoing in the early Universe. When interactions between a particle ψ and the rest of the plasma are efficient, the distribution function of the ψ species is well described by equilibrium distribution functions. Namely, fermions and bosons follow the usual Fermi-Dirac (FD) and Bose-Einstein (BE) distribution functions.

$$f_{FD} = \frac{1}{e^{(E-\mu)/T} - 1} \tag{1.18}$$

$$f_{BE} = \frac{1}{e^{(E-\mu)/T} + 1} \tag{1.19}$$

If scattering/annihilation/decay processes are not fully efficient, the distribution function of a given species may not exactly be described by a Fermi-Dirac or Bose-Einstein formula. However Escudero[2] showed that the relevant thermodynamic quantities can be tracked very accurately if we **assume that the species follow their equilibrium distribution at all times**. The advantage of this approximation is that we can find simple differential equations for the time evolution of the temperature and chemical potential that fully describe the thermodynamics of a given system.

1.3.3 Temperature and chemical potential evolution for a generic species

Multiplying 1.14 with $g\frac{d^3p}{2\pi^3}$ and $g\frac{d^3p}{2\pi^3}E$ and integrating gives

$$\frac{dn}{dt} + 3Hn = \frac{\delta n}{\delta t} = \int g\frac{d^3p}{2\pi^3}\mathscr{C}[f] \tag{1.20}$$

$$\frac{d\rho}{dt} + 3H(\rho + \mathscr{P}) = \frac{\delta \rho}{\delta t} = \int g\frac{d^3p}{2\pi^3}\mathscr{C}[f]E \tag{1.21}$$

By trivial use of chain rule, we can obtain

$$\frac{dn}{dt} = \frac{\partial n}{\partial T}\frac{dT}{dt} + \frac{\partial n}{\partial \mu}\frac{d\mu}{dt} \tag{1.22}$$

$$\frac{d\rho}{dt} = \frac{\partial \rho}{\partial T}\frac{dT}{dt} + \frac{\partial \rho}{\partial d\mu}\frac{\mu}{dt} \tag{1.23}$$

On rearranging terms we get,

$$\frac{dT}{dt} = \left(\frac{d\rho}{dt}\frac{\partial n}{\partial \mu} - \frac{dn}{dt}\frac{\partial \rho}{\partial \mu}\right) \Big/ \left(\frac{\partial n}{\partial \mu}\frac{\partial \rho}{\partial T} - \frac{\partial n}{\partial T}\frac{\partial \rho}{\partial \mu}\right) \tag{1.24}$$

$$\frac{d\mu}{dt} = \left(\frac{dn}{dt}\frac{\partial \rho}{\partial T} - \frac{d\rho}{dt}\frac{\partial n}{\partial T}\right) \Big/ \left(\frac{\partial n}{\partial \mu}\frac{\partial \rho}{\partial T} - \frac{\partial n}{\partial T}\frac{\partial \rho}{\partial \mu}\right) \tag{1.25}$$

We can substitute the above equations in 1.20 and 1.21, expressing the numerator in terms of Hubble's Rate, number and energy density

$$\frac{dT}{dt} = \frac{1}{\left(\frac{\partial n}{\partial \mu}\frac{\partial \rho}{\partial T} - \frac{\partial n}{\partial T}\frac{\partial \rho}{\partial \mu}\right)}\left[-3H\left((\rho + \mathscr{P})\frac{\partial n}{\partial \mu} - n\frac{\partial \rho}{\partial \mu}\right) + \frac{\partial n}{\partial \mu}\frac{\delta \rho}{\delta t} - \frac{\partial \rho}{\partial \mu}\frac{\delta n}{\delta t}\right] \tag{1.26}$$

$$\frac{d\mu}{dt} = \frac{-1}{\left(\frac{\partial n}{\partial \mu}\frac{\partial \rho}{\partial T} - \frac{\partial n}{\partial T}\frac{\partial \rho}{\partial \mu}\right)}\left[-3H\left((\rho + \mathscr{P})\frac{\partial n}{\partial T} - n\frac{\partial \rho}{\partial T}\right) + \frac{\partial n}{\partial T}\frac{\delta \rho}{\delta t} - \frac{\partial \rho}{\partial T}\frac{\delta n}{\delta t}\right] \tag{1.27}$$

These set of equations can be considerably simplified if chemical potentials are neglected. This typically occurs as a result of some efficient interactions. In the Standard Model, for example, efficient $e^+e^- \to \gamma\gamma$ and $e^+e^- \to \gamma\gamma\gamma$ interactions allow one to set $\mu_e(t) = \mu_\gamma(t) = 0$. If $\frac{d\mu}{dt} = 0$ then $\frac{dn}{dt} = \frac{d\rho}{dt}\frac{\partial n}{\partial T} / \frac{\partial \rho}{\partial T}$. This simplifies the 1.26 to

$$\frac{dT}{dt} = \frac{d\rho}{dt} \Big/ \frac{\partial \rho}{\partial T} \tag{1.28}$$

$$= \left[-3H(\rho + \mathscr{P}) + \frac{\delta \rho}{\delta t}\right] \Big/ \frac{\partial \rho}{\partial T} \tag{1.29}$$

1.3.4 Putting it together: Neutrino decoupling in SM using Escudero's Code

Using the above discussion we now write down the differential equations describing the time evolution of the temperature of the electromagnetic plasma T_γ and the neutrino fluid T_ν. We'll first summarise the approximatons used in writing these equations

- **All the species invloved (e^+, e^-, γ, ν) follow perfect equilibrium conditions**: This is the most fundamental assumption which stems from the fact that the non-thermal corrections to the equilibium distributions account for less that 1% of the total energy density of a species [2].
- **Neutrino Oscillations are neglected:** The effect of neutrino oscillations on $N_{\rm eff}$ is small ($\Delta N_{\rm eff}^{\rm SM} = 0.0007$) [3]. To approximately mimic the effect of neutrino oscillations the neutrino fluid is described with a single temperature, $T_\nu = T_{\nu_e} = T_{\nu_\mu} = T_{\nu_\tau}$.
- **The chemical potentials are neglected:** The photon number is not conserved in the early universe and the small baryon to photon ratio justifies setting $\mu_e = \mu_\gamma = 0$. The neutrino interactions $\nu\overline{\nu} \to e^+e^- \to \gamma\gamma$ are also highly efficient in the concerned temperature regime, justifying $\mu_\nu = 0$. However, it is explicitly checked that accounting for the neutrino chemical potential doesn't affect the results significantly.

We are now all set to write the temperature evolution equations. We consider the SM plasma and neutrinos separately. In the SM plasma e^-, e^+ are tightly coupled to the photons via efficient annihilations and scatterings during neutrino decoupling and thus share a common temperature $T_\gamma = T_e$. Thus we can write a common temperature evolution equation for the whole SM plasma using 1.29

$$\frac{dT_\gamma}{dt} = -\frac{4H\rho_\gamma + 3H(\rho_e + \mathscr{P}_e) - \frac{\delta\rho_e}{\delta t}}{\frac{\partial\rho_\gamma}{\partial T_\gamma} + \frac{\partial\rho_e}{\partial T_\gamma}} \tag{1.30}$$

where we've used that for photons $\mathscr{P} = \rho/3$ and the contribution to $\delta\rho/\delta t$ It comes only from electrons due to weak interactions with the neutrino sector. One interesting thing to note here is that the energy interchange b/w electrons and photons is so efficient that it doesn't let the temperatures of both sectors change and this is the reason why we can write a common evolution equation in the first place.

In the standard model, the total energy interchange b/w electrons and neutrinos must sum up to 0 as these are the only particles present.

$$\implies \frac{\delta\rho_e}{\delta t} + \frac{\delta\rho_{\nu_e}}{\delta t} + 2\frac{\delta\rho_{\nu_\mu}}{\delta t} = 0 \tag{1.31}$$

where the factor of 2 is because of identical energy transfer rates in case of μ and τ neutrinos. Substituing 1.31 into 1.30 we obtain

$$\frac{dT_\gamma}{dt} = -\frac{4H\rho_\gamma + 3H(\rho_e + \mathscr{P}_e) + \frac{\delta\rho_{\nu_e}}{\delta t} + 2\frac{\delta\rho_{\nu_\mu}}{\delta t}}{\frac{\partial\rho_\gamma}{\partial T_\gamma} + \frac{\partial\rho_e}{\partial T_\gamma}} \tag{1.32}$$

Finally a more accurate temperature evolution equation would also include the Linear Order (LO) and Non-Linear Order (NLO) finite temperature QED corrections as well to the electromagnetic energy and pressure densities. These corrections are denoted as $\mathscr{P}_{\text{int}}$ and $\rho_{\text{int}} = -\mathscr{P}_{\text{int}} + T_\gamma \frac{d\mathscr{P}_{\text{int}}}{dT_\gamma}$ and their values have been taken from [4]. This gives us the final temperature evolution equation for the photon plasma

$$\boxed{\frac{dT_\gamma}{dt} = -\frac{4H\rho_\gamma + 3H(\rho_e + \mathscr{P}_e) + 3HT_\gamma\frac{d\mathscr{P}_{\text{int}}}{dT_\gamma} + \frac{\delta\rho_{\nu_e}}{\delta t} + 2\frac{\delta\rho_{\nu_\mu}}{\delta t}}{\frac{\partial\rho_\gamma}{\partial T_\gamma} + \frac{\partial\rho_e}{\partial T_\gamma} + T_\gamma\frac{d^2\mathscr{P}_{\text{int}}}{dT_\gamma^2}}} \tag{1.33}$$

Similary we can write an equation for the neutrino sector consisting of all the three neutrino flavours

$$\boxed{\frac{dT_\nu}{dt} = -\frac{12H\rho_\nu - \frac{\delta\rho_{\nu_e}}{\delta t} - 2\frac{\delta\rho_{\nu_\mu}}{\delta t}}{3\frac{\partial\rho_\nu}{\partial T_\nu}}} \tag{1.34}$$

1.3.5 Results

We solve the above differential equations with an initial condition of $T_\gamma = T_\nu = 10MeV$. We also explicity check our assumption that neutrino chemical potential can be neglected by taking that into account. The difference b/w the is less than 0.02%. Hence our assumption is valid. In the next section we compare these results with the state of the art calculation and current and future experimental precision.

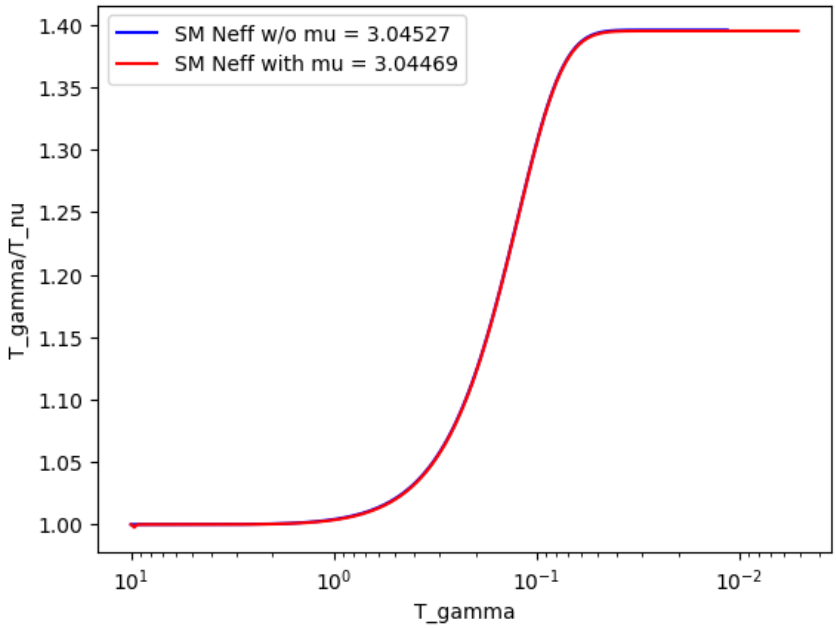

Figure 1.3: Results obtained using Escudero's Code

1.3.6 Comparison

Table 1.1: Comparison of N_{eff} = 3.045 obtained using Escudero's Code with other sources

Source/ Method	N_{eff}	% change
Instantaneous Decoupling	3	1.5 %
Salas Pastor et al[3] (State of the Art)	3.046	0.03 %
Current Precision (Planck 2018)	σ (N_{eff}) $\sim$ 0.2	5-6 %
Future Precision (Simons Observatory and CMB -S4)	σ (N_{eff}) $\sim$ 0.05	1-2 %

2. N_{eff} Measurements from CMB

In the last chapter we studied how we can theoretically calculate the value in the Standard Model case. But now the question arises, how do we verify this calculation? The answer to this question (like most other questions regarding the Primordial Universe) is given by the observations of Cosmic Microwave Background. CMB is an important source of data on the primordial universe. In this chapter, we'll first discuss how can we obtain the value burried inside the CMB measurements and later discuss how the upcoming advances in technology related to CMB measurements will significantly improve precision of the value.

2.1 CMB Power Spectrum: A qualitative description

The remarkable image in **??** is a snapshot of the universe when it was only 380,000 years old. It displays fluctuations in the intensity of CMB photons, which are a reflection of the density variations at the time of photon decoupling.

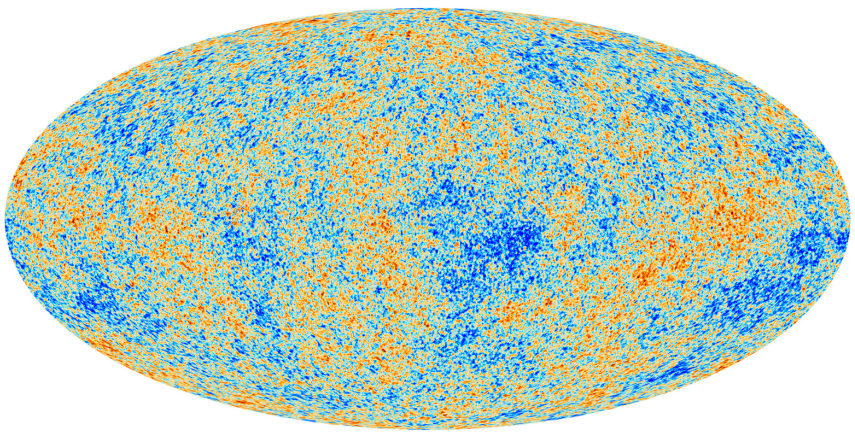

Figure 2.1: Temperature fluctuations in the cosmic microwave background as measured by the Planck satellite [5]

The CMB temperature fluctuations are analyzed statistically by measuring the correlations between hot and cold spots as a function of their angular separation. The result is the angular power spectrum shown in 2.2. The figure also shows a fit of the theoretical prediction for the CMB spectrum to the data. The agreement between the theory and the data is remarkable. A higher l

value represents a higher multipole and a lower angular scale.

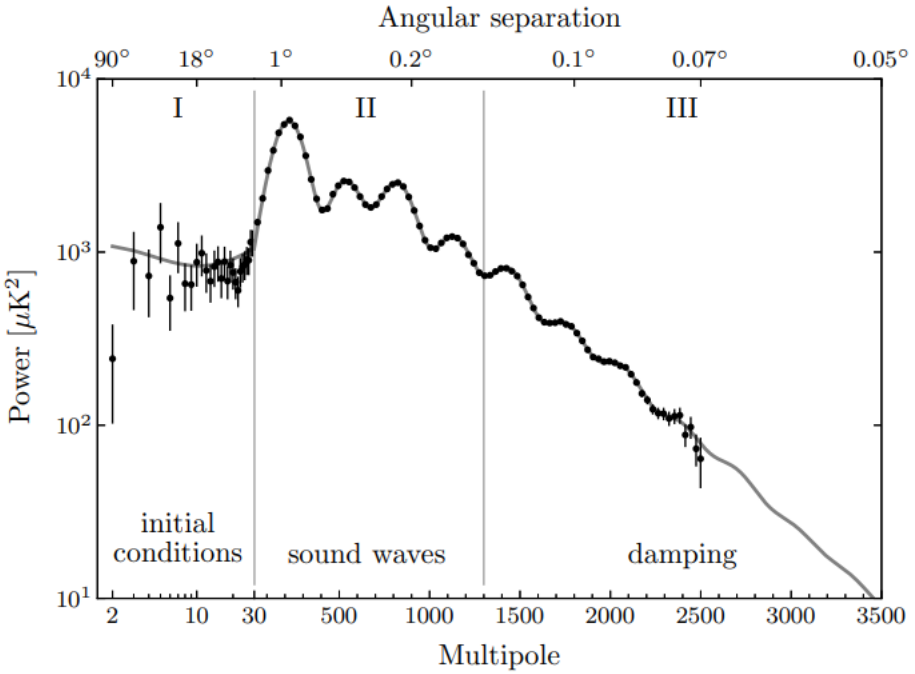

Figure 2.2: Planck 2018 Temperature Power Spectra [6]

Qualitatively, we can separate the CMB spectrum in three different regimes as shown in the figure above

- **Region I**: Correlations at large angles are caused by fluctuations that had not yet entered the horizon at the time of recombination. These fluctuations did not change before the photons were decoupled, thus providing a direct insight into the initial conditions.
- **Region II**: CMB perturbations with shorter wavelengths crossed the horizon before the recombination period. Inside the horizon, the perturbations in the tightly-coupled photon-baryon fluid moved as sound waves, which were sustained by the high photon pressure. The oscillation frequency of these waves is determined by their wavelength, so that different modes were captured at different points in their development when the CMB was released at photon decoupling. This is the source of the oscillatory pattern seen in the angular power spectrum of the CMB.
- **Region III**: At scales smaller than the average distance between photons, the random diffusion of the photons can cause the density contrast in the plasma to be eliminated, resulting in a decrease in the magnitude of the wave amplitudes. This has the effect of reducing the power of the CMB spectrum on small angular scales (high multipole moments)

Out of the three regions, the one of prime interest to us is the region III. The damping tails in the region are affected significantly (as compared to the other regions) by the amount of total radiation density before recombination. The SM radiation particles present in that era are neutrinos and photons. The total radiation density is thus given by

$$\rho_{\text{rad}} = \rho_\gamma + \rho_\nu = \left[1 + \frac{7}{8}\left(\frac{4}{11}\right)^{4/3} N_{\text{eff}}\right] \rho_\gamma \tag{2.1}$$

As we'll see in the next chapter, that we can tweak the definition of a little bit to incorporate other BSM degrees of freedom as well such that the above equation would still hold for finding the total

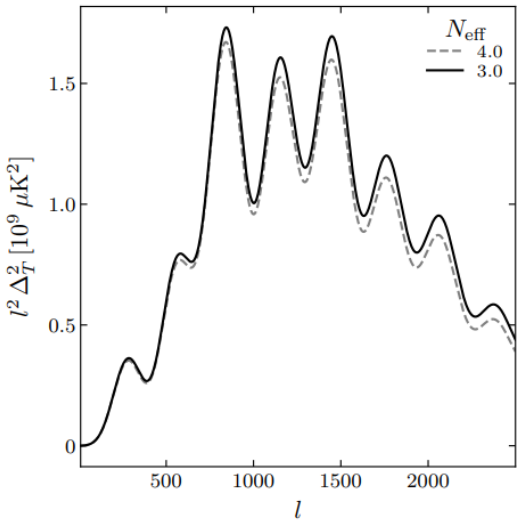

Figure 2.3: Variation of the CMB temperature power spectrum as a function of . The spectra have been multiplied by a factor of l^2 to emphasize the effects at large l

radiaton density.
Now in the above equation ρ_γ is fixed by the CMB Temperature, but there can be extra radiation density at the recombination due to some Beyond Standard Model (BSM) lightly coupled species. Thus gives us a direct measure of the radiation density at the time of recombination. In the figure below we can see how the value of affects the high multiple (small angular scales) spectrum of CMB.‘

As expected the damping is larger for a larger (larger radiation density). By using sophistictated fitting algorithms Planck Collaborators extracted out of these damping tails and the constraint they obtained is $= 2.99 \pm 0.17$. There are two important conclusions that can be drawn from this measurement

- Recall that the SM calculated in previous chapter was 3.045. The good news is that this value falls within the bounds predicted by Planck. However, from the current observations it is quite likely that the actual value differs from the pedicted SM value. This is where the theorists get excited! As this (possible) discrepancy b/w the observed and the predicted value implies that there's something more happening which is yet to be taken into account in order to correctly predict . One of the most popular resolution include involving some BSM degrees of freedom to predict correctly. In the next two chapters we've reviewd two such dark matter models.
- Clearly the current measurement is not precise enough to conclusively determine the presence or absence of additional degrees of freedom. Hence there have been ongoing efforts to improve the precision of the measurementsby next generation experiments. We'll discuss the implications and forecasts of one such experiment in the next section.

2.2 CMB-S4

CMB observations trace all the way back to 1964, when Penzias and Wilson accidently measured an everpresent unkown signal in their measurements to look for neutral hydrogen using a radio telescope at Bell Lab, New Jersey. In 1978 Penzias and Wilson were awarded the Nobel Prize for the discovery of the CMB. In 1989, NASA sent the Cosmic Background Explorer (COBE) into space, which verified earlier measurements of the CMB with remarkable precision in 1990. Two years later, it detected the anisotropies for the first time.

Since the launch of the Cosmic Background Explorer (COBE) satellite, two other CMB satellites have been used to map the entire sky. The first was the Wilkinson Microwave Anisotropy Probe (WMAP) which had a moderate angular resolution of up to 12 arcminutes. This was followed by the Planck satellite which had a resolution of up to 5 arcminutes. Additionally, ground-based experiments such as the 10m South Pole Telescope (SPT) and the 6m Atacama Cosmology Telescope (ACT) have provided higher-resolution maps of smaller regions of the sky.

CMB-S4[7] is the next-generation ground-based cosmic microwave background experiment. To get an idea about the improvement in the sensitivity, here's a plot showing the sensitivity of recent experiments, expectations for upcoming Stage-3 experiments, characterized by order 10,000 detectors on the sky, and the projection for a Stage 4 experiment with order 100,000 detectors

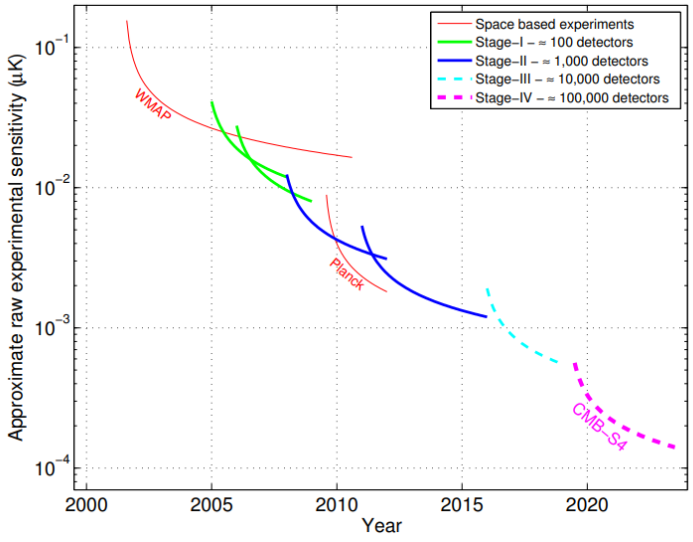

Figure 2.4: Sensitivity comparison of various CMB experiments

2.2.1 Impact of Improved Sensitivity on measurements

With the improved sensitivty and more precise mesurements at lower angular scales (higher multiploles), the conservative configurations of CMB-S4 can reach $\sigma() \sim 0.02$ - 0.03. What this means is that if $\Delta N_{\text{eff}} = N_{\text{eff}} - N_{\text{eff}}^{\text{SM}}$ is as small as 0.02 - 0.03, our observations would be able to precisely measure it. At these levels of sensitivity, CMB-S4 can reach a number of compelling targets for beyond the Standard Model (BSM) physics. Even in the absence of a detection, CMB-S4 would place constraints that can be orders of magnitude stronger than current probes of the same physics.

The parameter is an attractive theoretical target due to the fact that models of various kinds can be divided into two main levels of Δ. As demonstrated in Figure2.5, any species that was in thermal equilibrium with the Standard Model degrees of freedom will lead to a specific adjustment of Neff that is only dependent on its spin and its freeze-out temperature. If the freeze-out occurs after the QCD phase transition, then Δis at least 0.3. On the other hand, if the freeze-out happens before the QCD phase transition, then Δis at least 0.027. The first category has already been tested by the data from the Planck satellite. The second category, which is sensitive to freeze-out temperatures as high as the reheating temperature, can be explored by the CMB-S4.

The contributions to from hot thermal relics are relatively easy to understand from the discussion of neutrino decoupling in chapter 1. If we consider a hot thermal relic which decouples before

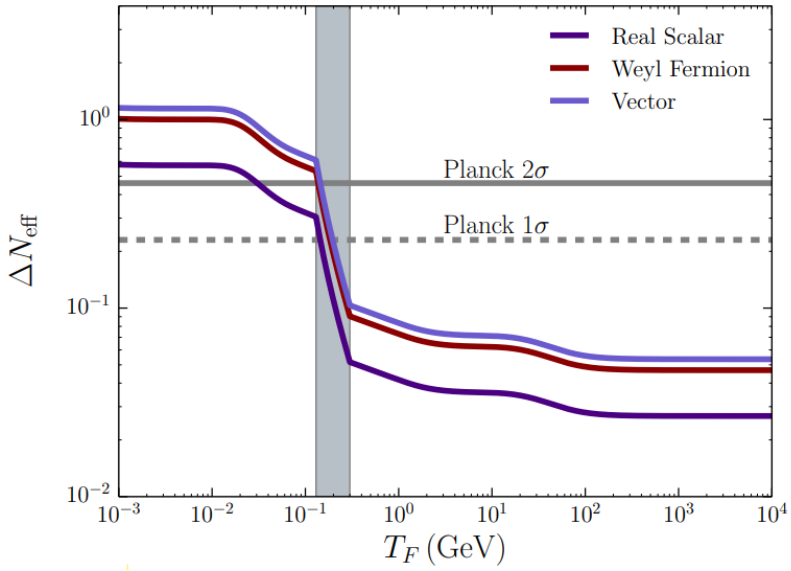

Figure 2.5: Contribution to from a massless field that was in thermal equilibrium with the Standard Model at temperatures T > T_F. Temperatures in the grey region correspond to the QCD phase transition.

neutrinos at a temperature T_F, then the temperature of such species just before neutrinos decouple can be obtained using the arguments of entropy conservation as follows

$$s_F a_F^3 = s_{\nu,decoup} a_{\nu,decoup}^3 \tag{2.2}$$

$$g_*(T_F) T_F^3 a_F^3 = g_*(T_{\nu,decoup}) a_{\nu,decoup}^3 T_{\nu,decoup}^3 \tag{2.3}$$

In the above equation g_* denotes total degrees of freedom, including an addition factor of 7/8 for fermions. Once the hot relic decouple, the only species that remain in the plasma are photons, neutrinos, elecctrons an positrons. As we calculated the contribution due to these species to g_* is 43/4. Also the temperature for hot relic dilutes as a^{-1} one it decouples. Hence the temperature of the hot relic at neutrino decoupling is given by

$$T_{\rm relic} = a_F T_F / a_{\nu,decoup} \tag{2.4}$$

$$\implies \left(\frac{T_{\rm relic}}{T_{\nu,decoup}}\right)^3 = \frac{43/4}{g_*(T_F)} \tag{2.5}$$

Once the neutrinos decouple this temperature ratio remains constant as both temperatures dilute as a^{-1}. As we can see from the equation 2.1, there is extra radiation density contributed due to this relic, resulting in Δ given by

$$\Delta N_{\rm eff} = \begin{cases} \frac{4g}{7}\left(\frac{43/4}{g_*(T_F)}\right)^{4/3} & \text{(boson)} \\ \frac{g}{2}\left(\frac{43/4}{g_*(T_F)}\right)^{4/3} & \text{(fermion)} \end{cases} \tag{2.6}$$

where g is the number of the independent spin states of the relic itself

The order of magnitude difference in Δ before and after the QCD phase transition comes from an order of magnitude drop in g_* below the QCD scale. The value of g_* above QCD scales is 106.75. We can then see from Eq. 2.6 that the minimum value of Δ for a single real scalar is 0.027, for a Weyl fermion is 0.047, and for a light vector boson is 0.054.

- $\Delta \geq 0.047$, for models containing additional light particles of spin 1/2, 1 and/or 3/2 A CMB experiment reaching $\sigma() \sim 0.02$ - 0.03 would be sensitive to all models in this very broad class of extensions of the Standard Model at 2σ, which includes any thermal population of gravitinos and dark photons.
- $\Delta \geq 0.027$ is predicted for models containing additional light particles of spin 0. A CMB experiment reaching $\sigma() \sim 0.02$ - 0.03 would be sensitive to all such models at 1σ, which includes a wide range of models predicting axions and axion-like particles.

3. BSM N_{eff}: Dark matter interacting with the SM via massive dark photons

3.1 The Model

In this chapter we study the impact of one particular dark matter(DM) model [8] on N_{eff}. The salient features of this model are

- A DM particle χ coupled to a massive dark photon A' that is kinetically mixed with the SM photon.
- A new inert, relativistic degree of freedom ξ, hereby referred to as the equivalent neutrinos

The model parameters include

- m_χ - mass of the DM particle
- $\Delta N_\nu = 3\rho_\xi/\rho_\nu$ - Change in N_{eff} contributed due to the equivalent neutrinos
- $m_{A'}/m_\chi$ - ratio of mass of the dark photon and the DM particle χ

3.2 Temperature Evolution Equations

Since the DM particle χ coupled to a massive dark photon A' which is mixed with SM photon, we can assume that the photns Dm particle and the dark photon A' share a common temperature T_γ and thus we can write one common equation for the DM particle and the photon sector. This way we don't need to take the interactions of DM with SM plasma separately.

$$\frac{dT_\gamma}{dt} = -\frac{4H\rho_\gamma + 3H(\rho_e + \mathscr{P}_e) + 3H(\rho_\chi + \mathscr{P}_\chi) + 3H(\rho_{A'} + \mathscr{P}_{A'}) + 3HT_\gamma \frac{d\mathscr{P}_{\text{int}}}{dT_\gamma} + \frac{\delta\rho_{\nu_e}}{\delta t} + 2\frac{\delta\rho_{\nu_\mu}}{\delta t}}{\frac{\partial\rho_\gamma}{\partial T_\gamma} + \frac{\partial\rho_e}{\partial T_\gamma} + \frac{\partial\rho_\chi}{\partial T_\gamma} + \frac{\partial\rho_{A'}}{\partial T_\gamma} + T_\gamma \frac{d^2\mathscr{P}_{\text{int}}}{dT_\gamma^2}} \tag{3.1}$$

The evolution equation for the neutrino sector remains the same

$$\frac{dT_\nu}{dt} = -\frac{12H\rho_\nu - \frac{\delta\rho_{\nu_e}}{\delta t} - 2\frac{\delta\rho_{\nu_\mu}}{\delta t}}{3\frac{\partial\rho_\nu}{\partial T_\nu}} \tag{3.2}$$

There's one additional component here, the equivalent neutrinos. Since these particles don't interact with any other species, their energy density scales as $\rho \propto a^{-4}$. For completeness, we write the evolution equation for these particles also,

$$\boxed{\frac{dT_\xi}{dt} = -\frac{4H\rho_\xi}{\frac{\partial\rho_\xi}{\partial T_\xi}}} \tag{3.3}$$

3.3 N_{eff} definition in Beyond Standard Model(BSM) Case

As discussed in chapter 2, the way N_{eff} is measured, it can be affected by all the extra relativistic species (not just neutrinos) except photons which were present at the time of photon decoupling. So we modify our original definition of N_{eff} to account for these extra relativistic species

$$\boxed{N_{\text{eff}} = \frac{8}{7}\left(\frac{11}{4}\right)^{4/3}\frac{\rho_{\text{rad}} - \rho_\gamma}{\rho_\gamma}} \tag{3.4}$$

In the SM case $\rho_{\text{rad}} = \rho_\nu + \rho_\gamma$ and thus we get back the original expression1.13

For the present DM scenario $\rho_{\text{rad}} = \rho_\nu + \rho_\gamma + \rho_\xi$

$$N_{\text{eff}} = \frac{8}{7}\left(\frac{11}{4}\right)^{4/3}\frac{\rho_\nu + \rho_\xi}{\rho_\gamma} \tag{3.5}$$

Since, we are following the assumption of equilibrium distribution, we can simplify the above expression further

$$N_{\text{eff}} = 3\left[\frac{11}{4}\left(\frac{T_\nu}{T_\gamma}\right)^3\right]^{4/3}\left(1 + \frac{\rho_\xi}{\rho_\nu}\right) \tag{3.6}$$

We relabel the ratio of the enrgy density contained in the equivalent neutrinos ρ_ξ and energy density of each flavour of the neutrino $\rho_\nu/3$ as ΔN_ν which gives us

$$\boxed{N_{\text{eff}} = 3\left[\frac{11}{4}\left(\frac{T_\nu}{T_\gamma}\right)^3\right]^{4/3}\left(1 + \frac{\Delta N_\nu}{3}\right)} \tag{3.7}$$

3.4 Results

Here are the results from the actual paper vs the results reproduced using our code for Planck . Of the three parameters of the model, we assumed $m_{A'}/m_\chi = 3$ with χ being a complex scalar and thus we obtained constraints on the other two parameters ΔN_ν and m_χ.

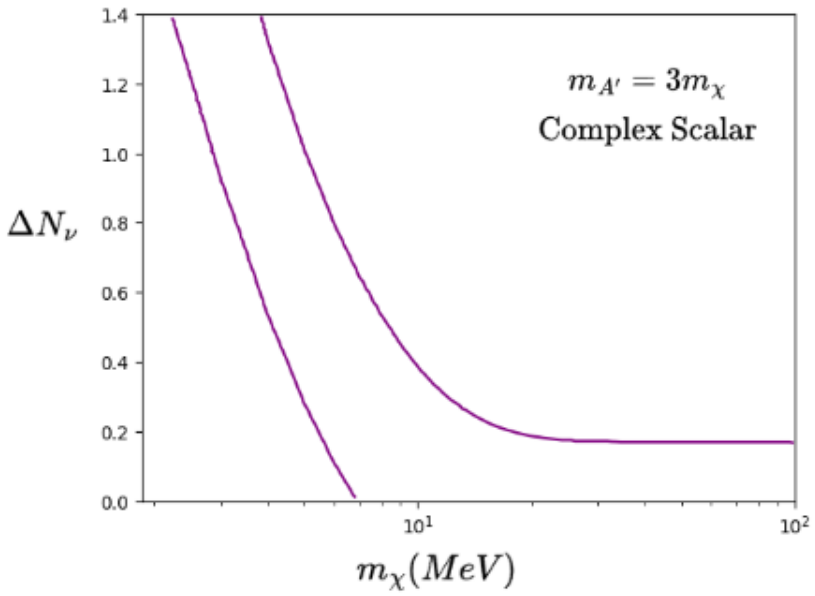

Figure 3.1: Planck N_{eff} constraints on the model (The region b/w the the two contours are the allowed set of parameter values, while the exterior region is excluded)

The following inferences can be drawn from the above plot

- At masses above approximately 20 MeV, the expected number of Neff approaches the standard cosmological value. This is because the Dark Matter (DM) freezes out before the neutrinos decouple, meaning that the DM annihilations heat the electromagnetic and neutrino sectors in the same way.
- . When the mass of the χ particle is less than 20 MeV, entropy is added to the electromagnetic sector during and after the neutrino decoupling period ($T_{\nu d} \sim 2$ MeV). This causes Neff to be lower than the standard value as the electromagnetic sector is heated more than usual. To bring Neff back to its observed value, a non-zero ΔN_{eff} must be present.

Bibliography

[1] Scott Dodelson. *Modern Cosmology*. 2003 (cited on page 6).

[2] Miguel Escudero Abenza. "Precision early universe thermodynamics made simple:neffand neutrino decoupling in the standard model and beyond". In: *Journal of Cosmology and Astroparticle Physics* 2020.05 (2020), pages 048–048. DOI: 10.1088/1475-7516/2020/05/048 (cited on pages 8, 9).

[3] Pablo F. de Salas and Sergio Pastor. "Relic neutrino decoupling with flavour oscillations revisited". In: *Journal of Cosmology and Astroparticle Physics* 2016.07 (July 2016), page 051. DOI: 10.1088/1475-7516/2016/07/051. URL: https://dx.doi.org/10.1088/1475-7516/2016/07/051 (cited on pages 9, 11).

[4] Jack J. Bennett et al. "Towards a precision calculation of the effective number of neutrinos Neff in the Standard Model: the QED equation of state". In: *Journal of Cosmology and Astroparticle Physics* 2020.03 (Mar. 2020), page 003. DOI: 10.1088/1475-7516/2020/03/003. URL: https://dx.doi.org/10.1088/1475-7516/2020/03/003 (cited on page 10).

[5] Planck Collaboration et al. "Planck 2018 results. VI. Cosmological parameters". In: 641, A6 (Sept. 2020), A6. DOI: 10.1051/0004-6361/201833910. arXiv: 1807.06209 [astro-ph.CO] (cited on page 13).

[6] Daniel Baumann. *Cosmology*. Cambridge University Press, June 2022. ISBN: 9781108838078. DOI: 10.1017/9781108937092. URL: http://dx.doi.org/10.1017/9781108937092 (cited on page 14).

[7] Kevork N. Abazajian et al. "CMB-S4 Science Book, First Edition". In: (Oct. 2016). arXiv: 1610.02743 [astro-ph.CO] (cited on page 16).

[8] Cara Giovanetti et al. "Joint Cosmic Microwave Background and Big Bang Nucleosynthesis Constraints on Light Dark Sectors with Dark Radiation". In: *Phys. Rev. Lett.* 129 (2 July 2022), page 021302. DOI: 10.1103/PhysRevLett.129.021302. URL: https://link.aps.org/doi/10.1103/PhysRevLett.129.021302 (cited on page 19).